http://dx.doi.org/10.18623/rvd.v22.n2.3155

FLEXURAL PERFORMANCE OF CONCRETE BEAMS INCORPORATING GRANITE WASTE

DESEMPENHO À FLEXÃO DE VIGAS DE CONCRETO INCORPORANDO RESÍDUOS DE GRANITO

Article received on: 2/13/2025
Article accepted on: 10/2/2025

Boukhari Ahmed*
*Department of Civil Engineering, Faculty of Architecture and Civil Engineering, University of Science and Technology of Oran Mohamed Boudiaf - USTO-MB (Oran 31000), Algeria
Sidi-Bel-Abbes 22000, Algeria
Orcid: https://orcid.org/0009-0003-8971-3698
ahmed.boukhari@univ-usto.dz

Driz Hafida **
**Department of Civil Engineering and Public Works, Faculty of Technologys, Djillali Liabes University, BP 89, Sidi Bel Abbes (22000), Algeria
Sidi-Bel-Abbes 22000, Algeria
Orcid: https://orcid.org/0009-0005-0968-3607
hafida.driz@univ-sba.dz

Rezagui Djihad ***
***Department of Hydraulics and Civil Engineering, Institute of Technology, University Centre of Maghnia (13000), Algeria
Maghnia, Algeria
Orcid: https://orcid.org/0009-0009-0328-5682
d.rezagui@cu-maghnia.dz

Benfrid Abdelmoutalib***
***Department of Hydraulics and Civil Engineering, Institute of Technology, University Centre of Maghnia (13000), Algeria
Maghnia, Algeria
Orcid: https://orcid.org/0009-0007-8171-1654
benfridabdelmoutalib2050@gmail.com

The authors declare that there is no conflict of interest

Abstract
This research examines the bending characteristics of a concrete beam reinforced with granite waste powder. The equilibrium equations are determined using an improved theory for deflection calculation, using the virtual work principle and the Navier solution technique. The Mori-Tanaka model is used to homogenize conventional concrete with different volumetric proportions of granite powder. This homogeneity enhances mechanical qualities like elastic modulus, shear resistance, and compressibility. The findings indicate that an augmentation in the volumetric percentage of granite powder reduces deflection and transverse displacement. The research delineates three principal advantages: improved mechanical performance of the beam, financial savings in construction via the use of granite waste, and

Resumo
Esta pesquisa examina as características de flexão de uma viga de concreto reforçada com pó de resíduo de granito. As equações de equilíbrio são determinadas utilizando uma teoria aprimorada para o cálculo da deflexão, utilizando o princípio do trabalho virtual e a técnica de solução de Navier. O modelo de Mori-Tanaka é utilizado para homogeneizar concreto convencional com diferentes proporções volumétricas de pó de granito. Essa homogeneidade aprimora qualidades mecânicas como módulo de elasticidade, resistência ao cisalhamento e compressibilidade. Os resultados indicam que um aumento na porcentagem volumétrica de pó de granito reduz a deflexão e o deslocamento transversal. A pesquisa delineia três vantagens principais: melhor desempenho mecânico da viga, economia financeira na

ecological benefits via the mitigation of dangerous gas emissions.

Keywords: Concrete Beam. Granite Waste. Flexural Behavior. Mori-Tanaka Model. Homogenization.

construção com o uso de resíduo de granito e benefícios ecológicos com a mitigação de emissões de gases perigosos.

Palavras-chave: *Viga de Concreto. Resíduo de Granito. Comportamento à Flexão. Modelo de Mori-Tanaka. Homogeneização.*

1 INTRODUCTION

Eco-friendly concretes are being increasingly used due to their reduced cost and capacity to diminish gas emissions. To improve concrete's mechanical qualities, this study investigates the use of granite debris as a partial cement replacement.

Initially, we will provide an overview of the CO_2 emissions generated by cement manufacturing. Jieru Zhang et al. develop a CO_2 accounting framework in the cement industry using LCA and alternative raw materials. The study analyses CO_2 emissions of concrete with low-carbon substitutions and proposes a methodology to optimize design and reduce environmental impacts [1]. Robbie M. et al. Andrew examine les émissions mondiales de CO_2 associées à la fabrication de ciment, représentant environ 4 % des émissions mondiales de combustibles fossiles. In 2018, emissions from cement manufacturing processes amounted to 1.50 ± 0.12 Gt of CO_2; 71% of these emissions have occurred since 1990 [2]. Song Nie et al. formulate a model to assess CO_2 emissions from low-carbon cement, demonstrating that calcium sufflaminate clinker (CSA) and HB-CSA produce lower CO_2 emissions than Portland cement. Utilizing supplemental cementitious materials (SCM) enhances emission reductions [3].

Studies have previously examined the reinforcement of concrete using granite. Sellaf Hamid and Hadj Mostafa Adda investigated using granite debris as a partial replacement for Portland cement. Owing to the effect of chloride ions on clinker hydration, hydrochloric acid influences the strength of concrete more significantly than sulfuric acid [4]. SURYA HADI investigates the impact of granite debris on the compressive strength of concrete. After 28 days, the compressive strength of standard concrete is 26.09 MPa, but the strengths of concrete, including 8%, 10%, and 12% granite waste, are 24.58 MPa, 22.69 MPa, and 21.28 MPa, respectively. This indicates that the inclusion of granite waste diminishes the compressive strength of concrete [5]. Debby Sinta Devi al investigate the use of rice husk ash and granite waste in concrete. The

optimal compressive strength findings (28.07 MPa) are achieved with 10% rice husk ash and 7.5% granite waste [6]. Bassel El Merabi et al. analyse dam foundation concrete-rock junction shear strength. The findings suggest a new roughness parameter since roughness factors do not directly affect shear strength [7]. Rahmani Farida et al. show that including granite powder as a partial substitute for Portland cement in self-compacting concrete preserves its qualities while reducing costs, CO_2 emissions, and valorizing waste [8]. B. Venkatesan et al. demonstrate that the correct incorporation of 15% granite powder and 30% glass powder enhances the performance of reactive powder concrete (RPC) performance, yielding superior chloride penetration resistance and delivering economic and ecological advantages [9]. Saravanan R et al. create resilient pavers by partly substituting cement with silica fume and sand with granite refuse. The findings indicate enhancements in strength and durability and a reduction in carbon emissions, offering a sustainable alternative for environmentally conscious buildings [10]. Alaa Mahmoud investigates using granite and marble waste powders as partial substitutes for cement in concrete. The findings indicate that 9% granite powder enhances compressive strength by as much as 33.2% at 800 °C, whilst 5% marble powder exhibits minor improvements. These tailored mixtures provide enhanced protection against gamma and neutron radiation; nevertheless, exposure to elevated temperatures diminishes shielding efficacy [11]. Hawraa Hasan Mousa demonstrates that recycled granite aggregates enhance compressive strength (from 33.6 to 43.9 MPa) and tensile strength, with a complete replacement elevating the strength to 36.9 MPa [12]. Sakthivel Rajendran investigates the use of granite waste and sea sand as substitutes for river sand in concrete production. Using 10% alccofine and 15% granite waste enhances the mechanical characteristics of concrete, resulting in substantial improvements in compressive, tensile, and flexural strength [13]. Adrien Chajec et al. examine the influence of granite powder waste on cementitious mixtures, emphasizing its beneficial effects on mechanical and functional characteristics. The report delineates research deficiencies, suggests future trajectories, and underscores the mitigation of costs and CO_2 emissions by using these wastes, concurrently enhancing the density of cement composites [14]. Vinicius Rodrigues dos Santos investigates using granite and marble debris in sustainable building materials via their integration into epoxy resin granite specimens. The findings indicate enhanced flexural strength, with the material displaying anisotropic characteristics and less environmental effect. Further investigation on resin optimization is required [15]. Talat

A. Bayoumi et al. developed a cement-granite composite matrix for managing radioactive waste. After 180 days of freeze-thaw cycles, the composite shows improved characteristics and is presented as a potential solution for radioactive waste solidification, requiring large-scale testing [16].

Numerous investigations have been conducted within the framework of homogenization theory and structural analysis. Benkabou et al. formulate a multi-scale numerical homogenization technique to forecast the elastoviscoplastic characteristics of high-performance concrete using finite element simulations and nanoindentation experiments. The findings derived from this methodology align with experimental data, therefore validating the method's dependability [17]. Chatbi et al. investigate the impact of silica nanoparticles on concrete slabs. The appropriate incorporation of SiO_2 enhances mechanical strength, whereas the elastic basis affects the bending behavior of the slabs [18]. Harrat et al. studied the static properties of concrete beams with nanosilica. The incorporation of SiO_2 improves mechanical characteristics by altering the microstructure. An analytical model indicates a decrease in deformations and stresses, highlighting the foundation's substantial impact on bending behavior [19]. Benfrid et al. examine the effects of glass powder on concrete exposed to thermomechanical stresses. Using the Eshelby model, their investigation delineates problems related to this inclusion and suggests modifications to enhance its efficacy [20]. Kecir et al. analyze the influence of Fe_2O_2 nanoparticles on the flexural behavior of concrete slabs with a non-local Eringen model. Their research indicates that a 30% concentration of Fe_2O_2 enhances elastic characteristics by 60% and reduces the deflection of thin slabs, affirming the capability of Fe_2O_2 nanoparticles to strengthen concrete constructions [21].

The predominant homogenization model referenced in the literature is the Mori-Tanaka model. Mori and Tanaka present a model to forecast the features of multilayer composite materials. This model correlates the microscopic attributes of the phases with their macroscopic qualities while considering their interconnections. This model is often used to examine multi-phase materials [22]. Mehmet Eker examines the elastic response of a functionally graded cylinder subjected to internal pressure using Mori-Tanaka homogenization. The boundary value issue is addressed using the Chebyshev technique, and the influence of the volume fraction index on stresses and displacements is analyzed [23]. Soheil Firooz determines a versatile interface model for heterogeneous materials, permitting alternative contact placements while preserving angular momentum

equilibrium. This model is included in the Mori-Tanaka approach for the analysis of reinforced composites, using FEM simulations to verify the analytical answers [24].

The computation algorithm for beam bending will be validated based on literature research concerning functionally graded beams (FGM). Khaled Meski et al. study the thermo-mechanical properties of a functionally graded beam using a higher-order shear deformation theory. The results are corroborated by traditional and advanced theories, with parametric analyses about the influence of geometries and mechanical characteristics [25]. Abdelbaki Chikh uses the Navier solution to examine the static characteristics of functionally graded beams (P-FGM). The numerical results from the novel shear models are juxtaposed with existing literature to evaluate the influence of geometry and the mixing rule [26]. Chitour Mourad et al. study the static behavior of functionally graded (FG) beams with simple supports using an advanced 2D shear deformation theory. The findings illustrate the theory's efficacy by comparing stresses and displacements across different parameters [27]. Bridjesh P examines the deformation of porous functionally graded beams (FGPB) by considering regular and irregular porosity distributions. The findings demonstrate the influence of porosity, volumetric fraction, and thickness ratios on the deflections and stresses of FGPB [28]. G. Chandra Mohana Reddy compares the deflection characteristics of bidirectional functionally graded porous beams, emphasizing both circular and straight configurations. The research examines these beams under various boundary conditions (SS, CC, CS) with mechanical loading, using a unified shear deformation theory to formulate deflection equations that include gradient material characteristics [29]. Geetha Narayanan Kannaiyan and Vivekanandam Balasubramaniam evaluate the bending characteristics of functionally graded porous beams (FGPB) with respect to both uniform and uneven porosity distributions. Numerical computations are conducted to ascertain maximal deflections, axial strains, and shear stresses, and the findings are compared to prior research for validation [30].

John A et al. study the variation in thickness in contact with reinforced concrete for a polymer reinforced with carbon nanotubes [31]. U.N. Wilson et al. study the bending of reinforced concrete structures in steel frameworks [32]. Charles Chinwuba Ike develops a model capable of studying beams in static bending, including shear deformation [33]. Charles Ike and Juliet Nneka Ugwu study buckling using a polygonal function to estimate the shear force [34]. Charles Ike examines the static bending of beams resting on strategic foundations using the theory that considers the effect of shear [35].

Turan, F. et al. study beams subjected to flexion-torsion with the HSDT method and introduce the effect of lateral shear with the beam-wall interaction [36]. Turan, F. et al. study the effect of buckling accompanied by torsion caused by a uniform load distribution with noticed orthotropy, including voids and shear deformation [37]. Albena Doicheva et al. study the force in beam-column connections [38]. Albena Doicheva et al. use finite elements to determine the interaction between beam and column in bending with detailed shear included in the operation [39]. Gao et al., in a detailed review of bending limits of beams [40], provide details on static bending and piezoelectric bending, with detailed comparisons [41]. MA Biot et al. were the first to use iterative methods in finite elements to study beam bending [42]. SP Xu adds the non-local effect to beam bending [43]. YM Yue et al. analyze microbeams based on Timoshenko's assumptions [44]. Liu, X. studies five-point bending for large beams using an analytical method [45]. To strengthen the idea of choosing the homogenization method, X. Wang et al. use the same Mori-Tanaka model to predict the elastic properties of concrete [46]. Y. Li et al. study the homogenization of concrete in a random medium [47]. Silva et al. examine high-performance concrete using Mori-Tanaka homogenization [48]. Zhou et al. [49] and Li, Y. [50] base their studies on Mori-Tanaka to determine the elasticity of concrete from various constituents and formulations.

This work investigates Mori-Tanaka homogenization to ascertain the mechanical characteristics of a concrete and granite powder combination, with volumetric percentages of cement ranging from 0% to 30% in increments of 10%. The validation of the calculation program is conducted using FGM parameters, and the improved theory is used to ascertain the deflection via the application of a high-order function, which represents the average of two functions to evaluate the shear effect. The findings indicate that marble powder enhances stiffness, thereby decreasing deflection.

2 MORI-TANAKA MODEL FOR HOMOGENIZATION

The composite material assumption that the sum of the volumes equals one.

$$V_m = 1 - V_c \quad \textbf{(1)}$$

The compressibility modulus, shear modulus, Young's modulus, and Poisson's ratio are correlated. These relationships are used to ascertain each material's compressibility and shear coefficients (concrete-granite powder).

$$K_m = \frac{E_m}{3(1-2\nu_m)}, \quad K_c = \frac{E_c}{3(1-2\nu_c)}, \quad G_m = \frac{E_m}{3(1+2\nu_m)}, \quad G_c = \frac{E_m}{2(1+\nu_c)} \qquad \textbf{(2)}$$

The effective modulus of bulk (Compressibility) (k) and shear (G) are given by:

$$\frac{K-K_m}{K_C-K_m} = \frac{V_c}{1+V_m\left(\frac{K_c-K_m}{K_m+\frac{4}{3}G_m}\right)} \qquad \textbf{(3)}$$

$$\frac{G-G_m}{G_C-G_m} = \frac{V_c}{1+V_m\left(\frac{G_c-G_m}{G_m+f1}\right)} \qquad \textbf{(4)}$$

Where:

$$f_1 = \frac{G_m(9K_m+8G_m)}{6(K_m+2G_m)} \qquad \textbf{(5)}$$

The effective modulus of elasticity E and Poissin's ratio ν are determined using the relation:

$$E = \frac{9KG}{3K+G}, \quad \nu = \frac{3K-2G}{2(3K+G)} \qquad (6)$$

It is noted that:

E: Homogeneous Elasticity Modulus.

K: Homogeneous Compressibility Modulus.

G: Homogeneous Shear Modulus.

Em: Matrix Elasticity Modulus.

Ec: Composite Elasticity Modulus.

Km: Matrix Compressibility Modulus.

Kc: Composite Compressibility Modulus.

Gm: Matrix Shear Modulus.

Gc: Composite Shear Modulus.

Vm: Matrix Volume.

Vc: Composite Volume.

vm: Matrix Poisson's Ratio.

vc: Composite Poisson's Ratio.

This study assumes the incorporation of marble powder into standard concrete. Post-homogenization, the material is considered as isotropic **(Figure 1.)** shows the homogenization diagram

Figure 1

The steps of homogenization between ordinary concrete and granite powder.

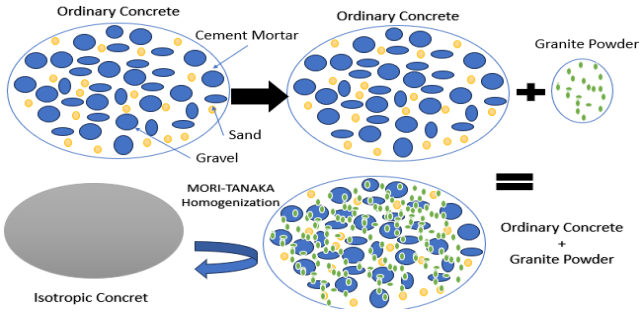

3 MATHEMATICAL MODEL FOR CALCULATING BENDING

The displacement field is written in the form of the refined theory.

Tapez une équation ici.

$$u_1(x,z,t) = u(x,z,t) - z\frac{dw_b}{dx} - f(z)\frac{dw_s}{dx}\; u_2(x,z,t) = 0 ; u_3(x,y,z_{ns},t) = w_b(x,t) + w_s(x,t)$$

(7)

The deformation and distortion are defined as: follows:

$$\varepsilon_x = \frac{du}{dx} + z\frac{\partial^2 w_b}{\partial x^2} - f\frac{\partial^2 w_s}{\partial x^2} ; \gamma_{xz} = \left(1 - \frac{df}{dz}\right)\frac{dw_s}{dx} = g\frac{dw_s}{dx} \qquad (8)$$

Noted that:

$$f = 0.67z^3 + 0.5z - 0.16\sin(\pi z) \qquad (9)$$

Where:

$$g = 1 - \frac{df}{dz} \qquad \textbf{(10)}$$

The equations of motion with virtual principal

$$\int_{-h/2}^{h/2}\int_{\Omega}\left[\sigma_x \delta\varepsilon_x + \tau_{xz}\delta\gamma_{xz}\right]d\Omega w dz - \int_{\Omega} q\delta w d\Omega = 0 \qquad \textbf{(11)}$$

The variation of deformation is defined as follows:

$$\delta U = \int_0^L \int_A (\sigma_x \delta\varepsilon_x + \tau_{xz}\delta\gamma_{xz}) dA dx = \int_0^L \left(N \frac{d\delta_u}{dx} - M_b \frac{d^2\delta w_b}{dx^2} - M_s \frac{d^2\delta w_s}{dx^2} + Q \frac{d\delta w_s}{dx} \right) dx \quad \textbf{(12)}$$

The variance of the potential

$$\delta V = -\int_0^L q\delta(w_b + w_s) dx \quad \textbf{(13)}$$

The resultant forces, moments, and shear forces are designated as follows:

$$N = \int_A \sigma_x dA \;\; N_b = \int_A z\sigma_x dA \;\; M_S = \int_A f(z)\sigma_x dA \;\; Q = \int_A g(z)\tau_{xz} dA \quad (14)$$

By replacing (13) in (11) the equilibrium equations are written:

$$\delta u : \frac{dN}{dx} = 0$$
$$\delta w_b : \frac{d^2 M_b}{dx^2} + q = 0$$
$$\delta w_s : \frac{d^2 M_s}{dx^2} + \frac{dQ}{dx} + q = 0 \quad \textbf{(15)}$$

The boundary conditions

$$w_b or Q_b = \frac{dM_b}{dx}$$
$$w_s or Q_s = \frac{dM_s}{dx} + Q$$
$$\frac{dM_b}{dx} or M_b$$
$$\frac{dM_s}{dx} or M_s \quad \textbf{(16)}$$

The relationship between constraint and deformation is defined as follows:

$$\sigma_x = Q_{11}\varepsilon_x \; ; \; \tau_{xz} = Q_{55}\gamma_{xz} \qquad \textbf{(17)}$$

Where:

$$Q_{11} = E$$

$$Q_{55} = \frac{E}{2} + [1+\nu] \qquad \textbf{(18)}$$

By substituting:

$$N = A\frac{du}{dx} - B\frac{d^2w_b}{dx^2} - B_s\frac{d^2w_s}{dx^2} \; ; \; M_b = B\frac{du}{dx} - D\frac{d^2w_b}{dx^2} - D_s\frac{d^2w_s}{dx^2} \qquad (19)$$

$$M_s = B_s\frac{du}{dx} - D_s\frac{d^2w_b}{dx^2} - H_s\frac{d^2w_s}{dx^2} \; ; \; Q = A_s\frac{dw_s}{dx} \qquad \textbf{(20)}$$

With:

$$A = \int_A Q_{11}dA \; ; \; B = \int_A zQ_{11}dA \; ; \; B_s = \int_A f(z)Q_{11}dA \; ; \; D = \int_A z^2 f(z)Q_{11}dA \qquad (21)$$

$$D_s = \int_A z\ f(z)Q_{11}dA \; ; \; H_s = \int_A f^2(z)Q_{11}dA \; ; \; A_s = \int_A g^2(z)Q_{55}dA \qquad \textbf{(22)}$$

Equation of motion:

$$D_s = \int_A z\ f(z)Q_{11}dA \; ; \; H_s = \int_A f^2(z)Q_{11}dA \; ; \; A_s = \int_A g^2(z)Q_{55}dA \qquad \textbf{(23)}$$

$$B\frac{d^3u}{dx^3} - D_s\frac{d^4w_b}{dx^4} - H_s\frac{d^4w_s}{dx^4} + A_s\frac{d^2w_s}{dx^2} + q = 0 \qquad (24)$$

Analytical solution (Navier):

$$u(x,t) = \sum_{n=1}^{\infty} U_n \cos(\alpha x) \quad ; \quad w_b(x,t) = \sum_{n=1}^{\infty} W_{bn} \sin(\alpha x) \quad ; \quad w_s(x,t) = \sum_{n=1}^{\infty} w_{sn} \sin(\alpha x) \qquad (25)$$

Where:

$$\alpha = \frac{n\pi}{L}, (U_n, W_{bn}, W_{sn}) \qquad \textbf{(26)}$$

Usining Fourier series:

$$q(x) = \sum_{n=1}^{\infty} Q_n \sin(\alpha x) \qquad \textbf{(27)}$$

Where load amplitude noted by:

$$Q_n = \frac{2}{L}\int_0^L q(x)\sin(\alpha x)dx \qquad \textbf{(28)}$$

The coefficients Qn are given calculated from:

$$Q_n = \frac{4q_0}{n\pi}(n = 1,3,5,....) \qquad \textbf{(29)}$$

for a uniform load

By replacing (23) in (24) the stiffness matrix noted:

$$\begin{bmatrix} S_{11} & S_{12} & S_{13} \\ S_{21} & S_{22} & S_{23} \\ S_{13} & S_{23} & S_{33} \end{bmatrix} \begin{Bmatrix} U_n \\ W_{bn} \\ W_{sn} \end{Bmatrix} = \begin{Bmatrix} 0 \\ Q_n \\ Q_{sn} \end{Bmatrix} \quad \textbf{(30)}$$

$$S_{11} = A\alpha^2,\ S_{12} = B\alpha^3,\ S_{13} = B_s\alpha^3,\ S_{22} = D\alpha^4,\ S_{23} = D_s\alpha^4,\ S_{33} = H_s\alpha^4 + A_s\alpha^2$$

(31)

The dimensional parameters are written in this formula:

$$w = 100\frac{E_m h^3}{q_0 L^4} w\left(\frac{L}{2}\right) \quad , \quad u = 100\frac{E_m h^3}{q_0 L^4} u\left(0, -\frac{h}{2}\right) \quad \sigma_x = \frac{h}{q_0 L}\sigma_x\left(\frac{L}{2}, \frac{h}{2}\right)$$

$$\tau_{xz} = \frac{h}{q_0 L}\sigma_{xz}(0,0) \quad \textbf{(32)}$$

4 RESULTS AND DISCUSSION

4.1 Mori-tanaka homogenization

The matrix comprises standard (ordinary) concrete, while the reinforcement consists of granite powder. The mechanical properties, including the modulus of elasticity (E) and Poisson's ratio (v), are evaluated. See (**Table 1**.) It is noted that all mechanical properties improve as the volume fraction increases, as shown in **(Figure 2.)** This evolution indicates that marble powder is a good addition to the ordinary concrete matrix. It results in a 15% increase in all mechanical properties, which automatically affects the rigidity of this new concrete.

Table 1

The properties of the materials used.

The mechanical properties	Ordinary Concrete [18]	Granite Powder [30]
Modulus of Elasticity (*E*) [GPa]	20	0.2
Poisson's ratio (*v*)	60	0.28

Figure 2

Elastic Modulus as a function of the volume fraction variation post-homogenization.

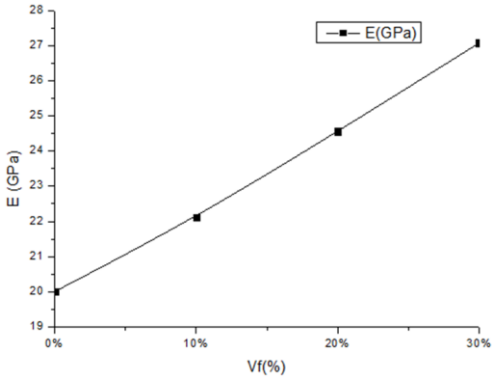

Figure 3

Post-Homogenization Poisson's Ratio as a Function of Volume Fraction.

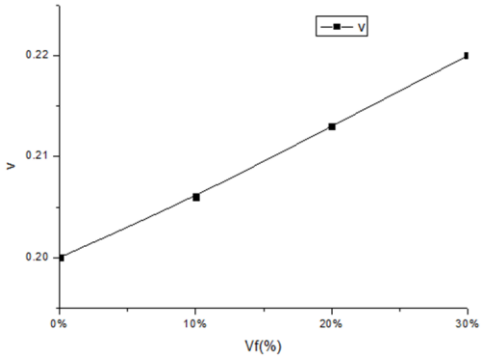

Figure 4

Dependence of Shear Modulus on Volume Fraction Post-Homogenization

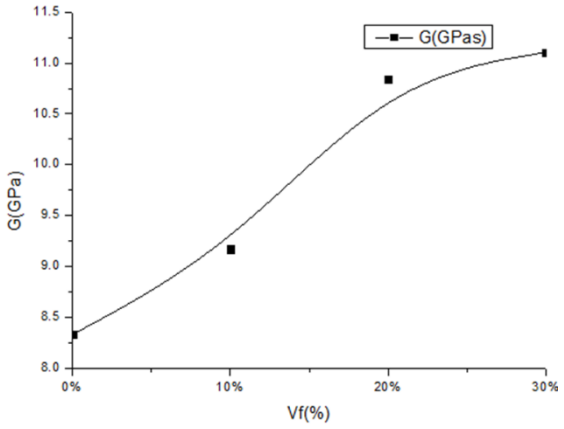

Figure 5

Variation of Bulk Modulus with Volume Fraction Following Homogenization.

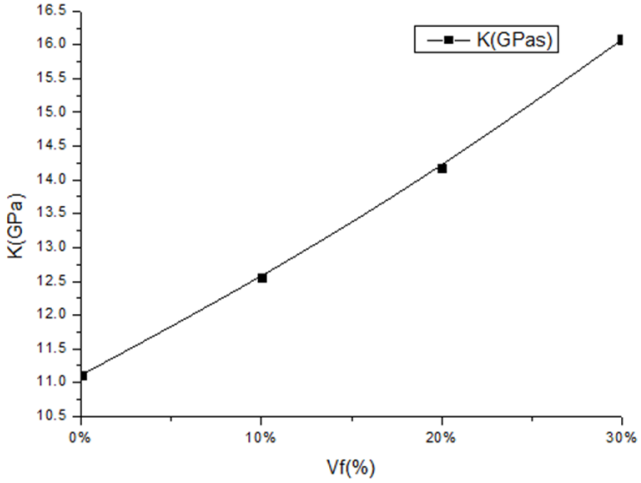

4.2 Validation of calculations

To validate the bending calculation software for the beam utilizing advanced theories, a comparison with a functionally graded material of power 0 was essential. The comparison between various analytical models is shown in **(Table 2.)**

This model is a close approximation and will be used to deduce the bending parameters for a beam of concrete reinforced with granite powder.

Table 2

Validation of the model and the HSDT function used for the bending of FGM beams with power 0.

The model	Transverse Displacement u	Deflection w	Normal Stress σ
Chitour Mourad et al [27]	0.9375	3.1643	3.7954
Present	0.9394	3.1686	3.7963

4.3 Flexural behavior of concrete beams reinforced with granite powder

Transverse displacement when l=5h, as shown in Fig 6, decreases as the granite powder content increases for ordinary concrete (approximately ±5.0075). The displacement decreases by about 0.5 when 10% granite powder is added. As the volume fraction increases, the transverse displacement decreases, as shown in Fig 7 for a geometric ratio l=10h, with a reduction of 0.23 for each 10% increment of granite powder.

In Fig8, for the geometric variation l=15h. The transverse displacement diminishes. of 0.15 for each 10% increase in granite powder. For Fig 6, 7, and 8, The displacement passes through zero with a symmetric value on either side. The transverse displacement cancels at the center of the beam and becomes positive on one side and negative on the other. This results in the bending effect, where one side is in tension, and the other is in compression. As the geometric parameter of the concrete beam grows, the transverse displacement diminishes, and the rate of reduction owing to the incorporation of granite powder becomes less pronounced. This indicates that the shear effect, which causes transverse displacement, will be insignificant in slender beams, unlike the problem observed in short beams.Fig9 illustrates the deflection of a short beam. The deflection of standard concrete with the specified dimensions is 17.17, while the deflections for concrete reinforced with 10%, 20%, and 30% granite powder are 14.77, 14.06, and 12.7, respectively, at the middle of the beam, with zero deflection at the ends. The deflections diminish as the volume fraction declines, indicating that granite powder substantially enhances concrete reinforcing. A marginal rise in everyday stress, while negligible, concerns the fifth decimal place. Consequently, the graphs in Fig 10 have some overlap. With an accuracy of five decimal places, granite powder somewhat elevates the typical stress. This graphic exhibit symmetry as traction and compression occur during the transition through zero. The tangential stress depicted in Fig 11 reaches its maximum in the beam's center, while the values at the ends are zero. The alteration will be depicted

in the third decimal place, indicating a reduction as the granite powder content escalates. Fig 10 and 11 clearly depict the issue with concrete pieces' bending impact. The rigidity of the beams is shown to increase with the incorporation of granite powder. The enhancements are substantial owing to the augmentation of mechanical qualities resulting from the incorporation of granite powder. Fig 12 indicates that an increase in beam length correlates with an increase in stress for narrow beams. This is rational, given that the beam's fragility escalates with an increase in span.

In Fig13, it is shown that the shear deformation remains almost the same. However, in Fig 14, it is observed that the addition of granite powder significantly reduces the deflection

Figure 6

Transverse Displacement u for Uniform Loading with Geometric Parameters a=h and l=5h for Eco-Concrete Reinforced by 10%, 20%, and 30% with Granite Powder, Compared to Ordinary Concrete

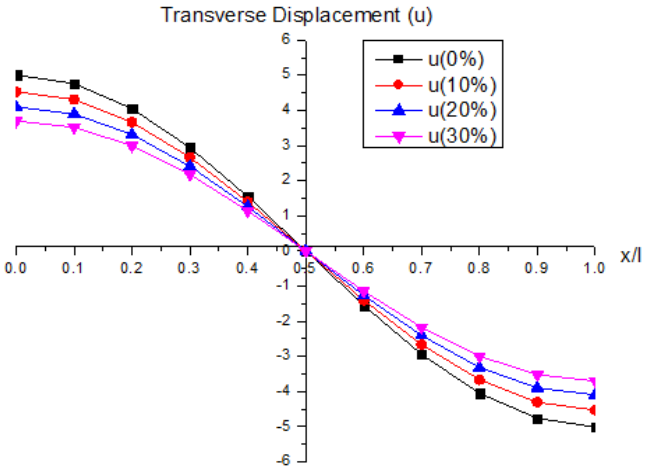

Figure 7

Comparison of Transverse Displacement u under Uniform Loading for Eco-Concrete Reinforced by 10%, 20%, and 30% with Granite Powder, with Ordinary Concrete, with Geometrical Parameters a=h and l=10h.

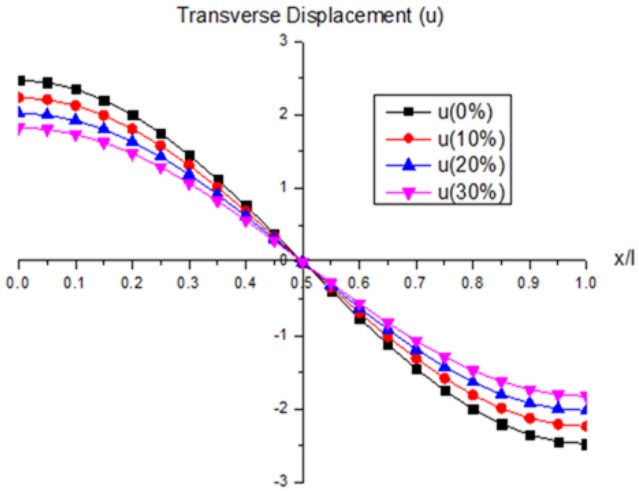

Figure 8

Effect of Reinforcement Levels (10%, 20%, 30%) with Granite Powder on Transverse Displacement u in Eco-Concrete and Conventional Concrete, with Geometric Parameters.

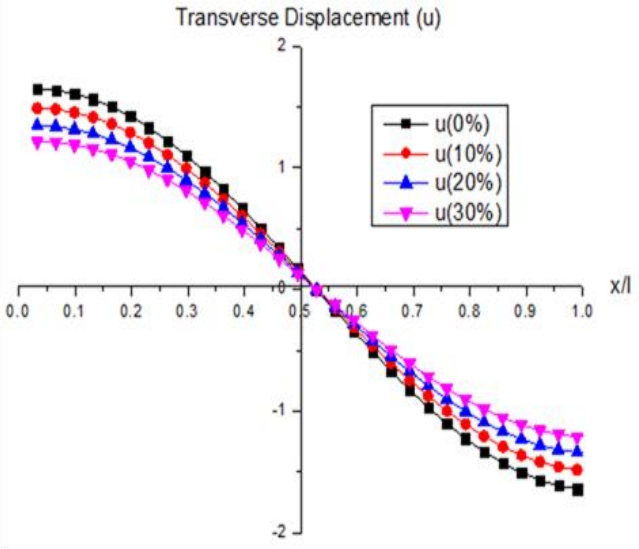

Figure 9

Deflection w under Uniform Loading with Geometric Parameters a=h and l=5h for Eco-Concrete Reinforced by 10%, 20%, and 30% with Granite Powder, Compared to Ordinary concrete.

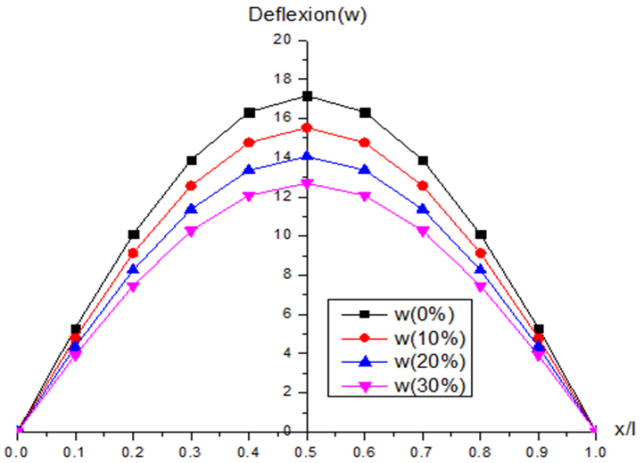

Figure 10

Normal Stress σ under Uniform Loading with Geometric Parameters a=h and l=5h for Eco-Concrete Reinforced by 10%, 20%, and 30% with Granite Powder, Compared to Ordinary concrete.

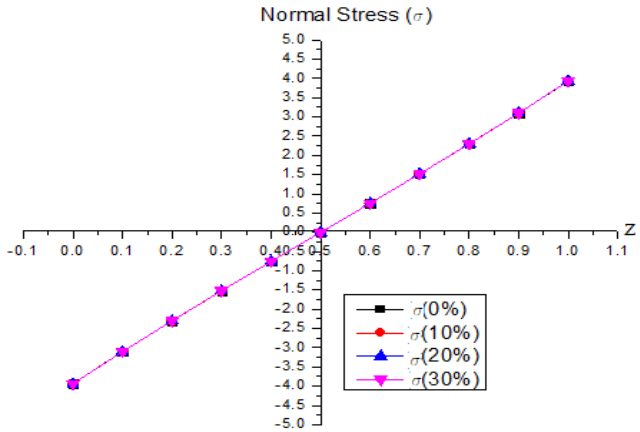

Figure 11

Shear Stress τ *under Uniform Loading with Geometric Parameters a=h and l=5h for Eco-Concrete Reinforced by 10%, 20%, and 30% with Granite Powder, Compared to Ordinary concrete.*

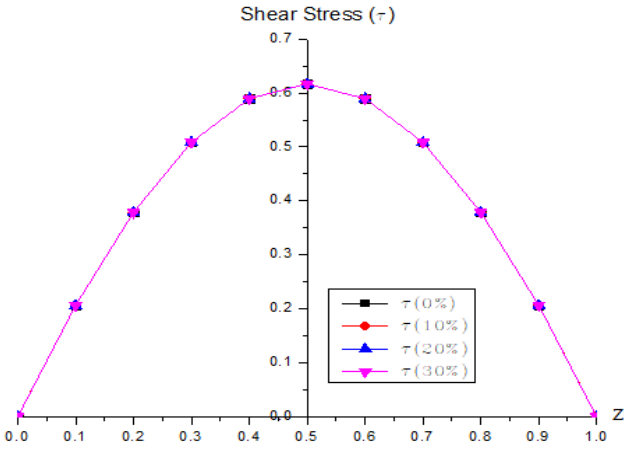

Figure 12

Normal Stress σ for Eco-Concrete Reinforced by 30% with Granite Powder, with Geometries a= and l=5h,10h,15h.

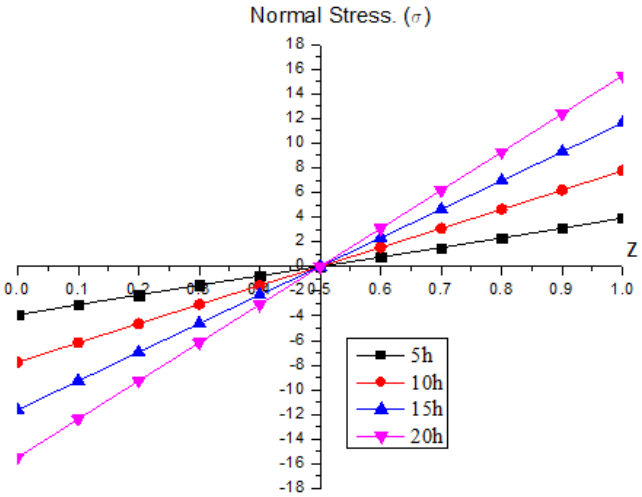

Figure 13

Normal Stress σ for Eco-Concrete Reinforced by 30% with Granite Powder, with Geometries a= and l=5h,10h,15h.

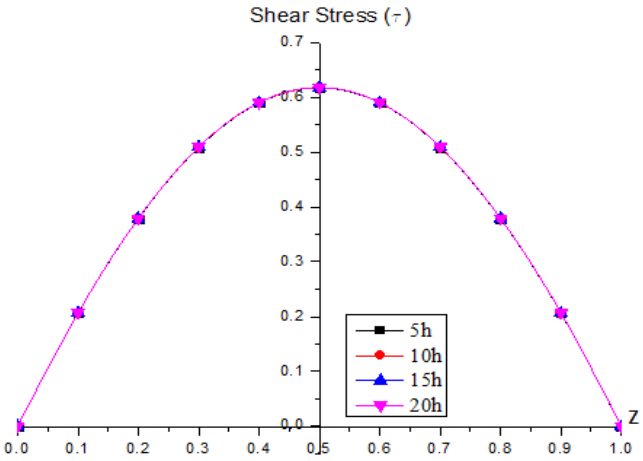

Figure 14

Maximum Deflection at Midspan of a Beam for Concrete Reinforced with Granite Powder and Ordinary Concrete.

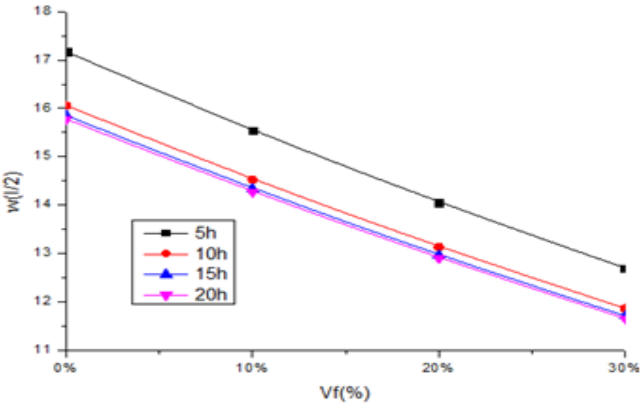

5 CONCLUSION

The research indicates that using granite powder in conventional concrete markedly improves its mechanical properties, notably the modulus of elasticity and Poisson's ratio. The incorporation of granite powder, namely within the 10% to 30% range, significantly enhances the stiffness of concrete beams, evidenced by less transverse displacement and deflection. The results indicate that granite powder enhances mechanical characteristics by 15%, increasing the beam's resistance to bending.

With an increase in the volume fraction of granite powder, both transverse displacement and deflection diminish. This impact is more prominent in short beams but diminishes in slender beams. The symmetry of the transverse displacement signifies that the beam undergoes a bending action, with one side under tension and the opposite side under compression.

Granite powder marginally elevates normal and tangential stresses, particularly in finer decimal values. Moreover, it substantially diminishes the deflection of concrete beams, enhancing the material's overall strength and stability.

Granite powder is a sustainable and economical reinforcement, mitigating environmental impact while offering a cost-effective alternative to concrete. This method corresponds with contemporary trends in sustainable construction, rendering it a viable option for future applications.

REFERENCES

[1] F. Belaïd, "How does concrete and cement industry transformation contribute to mitigating climate change challenges?" Resources, Conservation & Recycling Advances, vol. 15, p. 200084, 2022.

[2] R. M. Andrew, "Global CO_2 emissions from cement production, 1928–2018," Earth Syst. Sci. Data, vol. 11, pp. 1675–1710, 2019.

[3] S. Nie, J. Zhou, F. Yang, M. Lan, J. Li, Z. Zhang, Z. Chen, M. Xu, H. Li, and J. G. Sanjayan, "Analysis of theoretical carbon dioxide emissions from cement production: Methodology and application," Journal of Cleaner Production, vol. 334, p. 130270, 2022.

[4] H. Sellaf and H. M. Adda, "Évaluation et performances des bétons incorporant de la poudre de granite comme substitution partielle du ciment dans des milieux agressifs," Revue des matériaux et énergies renouvelables, vol. 4, no. 1, pp. 22-28, 2020.

[5] S. Hadi, "Pengaruh Penambahan Limbah Granit Terhadap Kuat Tekan Beton," Ganec Swara, vol. 14, no. 1, pp. 476-480, 2020.

[6] D. S. Devi, R. Nurmeyliandari, and A. P. Pramadona, "Pengaruh Penggunaan Abu Sekam Padi dan Limbah Granit Terhadap Kuat Tekan Beton," Borneo Engineering: Jurnal Teknik Sipil, vol. 8, no. 1, 2024.

[7] B. El Merabi, M. Briffaut, and F. Dufour, "Étude expérimentale pour l'évaluation de la résistance au cisaillement de joints cohésifs rugueux de granite-béton," Annales de la Jeune Recherche en Génie Civil, vol. 35, no. 1, pp. 241–244, 2017.

[8] F. Rahmani, O. Haddad, and S. Kaci, "Influence de la Poudre de Granit sur le Comportement Mécanique et Rhéologique du Béton Autoplaçant."

[9] B. Venkatesan et al., "Ajout optimal de poudre de granit et de poudre de verre pour améliorer les performances du béton réactif (RPC)."

[10] R. Saravanan, K. Dhivash, M. D. Sugunthan, and M. Susirajamugan, "Sustainable Paver Block Development Using Silica Fume and Granite Waste," International Journal of Scientific Research in Engineering and Management, vol. 9, no. 04, pp. 1-9, 2025.

[11] A. Mahmoud, A. A. Elsayed, A. M. Aboraya, I. M. Nabil, A. Shokry, and others, "Elevated temperature effects on the compressive strength and radiation shielding capability of waste granite and marble concrete," The European Physical Journal Plus, vol. 140, no. 4, 2025.

[12] H. Mousa, A. A. Kadhem, H. S. Al-Bahrani, L. A. Mahdi Alasadi, and others, "Study The Re-Use of Construction and Demolition Waste for Friendlier Environment: Waste Concrete and Waste Granite Aggregates," Civil and Environmental Engineering, vol. 20, no. 2, pp. 711-719, 2024.

[13] S. Rajendran and R. Kanagaraj, "Experimental investigation on granite waste and alccofine in concrete," Matéria (Rio de Janeiro), vol. 28, no. 4, 2023.

[14] S. Raman and R. Nateriya, "Synthesizing sustainable construction paradigms: A comprehensive review and bibliometric analysis of granite waste powder utilization and moisture correction in concrete," Reviews on Advanced Materials Science, vol. 63, no. 1, 2024.

[15] V. Rodrigues dos Santos, L. M. Genova, S. M. Soares, D. Ribeiro do Carmo, and others, "Experimental study of the production of resin granite and marble using their solid waste," Matéria (Rio de Janeiro), vol. 29, no. 1, p. 1, 2024.

[16] T. A. Bayoumi, M. E. Tawfik, and S. B. Eskander, "Potential applications of granite-cement composite based on granite powder waste for radioactive wastes solidification: Impact of freezing-thawing treatment."

[17] R. Benkabou, B. Abbès, F. Abbès, A. Asroun, and Y. Li, "Contribution of 3D numerical simulation of instrumented indentation testing in the identification of elastic-viscoplastic behaviour law of a high-performance concrete," Matériaux & Techniques, vol. 105, no. 1, p. 102, 2017.

[18] M. Chatbi, B. Krour, M. A. Benatta, Z. R. Harrat, S. Amziane, and M. B. Bouiadjra, "Bending analysis of nano-SiO2 reinforced concrete slabs resting on elastic foundation," Structural Engineering and Mechanics, An Int'l Journal, vol. 84, no. 5, pp. 685-697, 2022.

[19] Z. R. Harrat, S. Amziane, B. Krour, and M. B. Bouiadjra, "On the static behavior of nano SiO_2 based concrete beams resting on an elastic foundation," Computers and Concrete, vol. 27, no. 6, pp. 575-583, 2021.

[20] A. Benfrid, A. Benbakhti, Z. R. Harrat, M. Chatbi, B. Krour, and M. B. Bouiadjra, "Thermomechanical analysis of glass powder based eco-concrete panels: Limitations and performance evaluation," Periodica Polytechnica Civil Engineering, vol. 67, no. 4, pp. 1284-1297, 2023.

[21] A. Kecir, M. Chatbi, Z. R. Harrat, M. B. Bouiadjra, M. Bouremana, and B. Krour, "Enhancing the mechanical performance of concrete slabs through the incorporation of nanosized iron oxide particles (Fe_2O_3): Non-local bending analysis," Periodica Polytechnica Civil Engineering, vol. 68, no. 3, pp. 842-858, 2024.

[22] T. Mori and K. Tanaka, "Average stress in matrix and average elastic energy of materials with multi-phase structure," Journal of the Mechanics and Physics of Solids, vol. 21, no. 5, pp. 273-274, 1973.

[23] M. Eker, D. Yarımpabuç, A. Yıldırım, and K. Çelebi, "Elastic solutions based on the Mori-Tanaka scheme for pressurized functionally graded cylinder," Journal of Applied Mathematics and Computational Mechanics, vol. 19, no. 4, pp. 57-68, 2020.

[24] S. Firooz, G. Chatzigeorgiou, P. Steinmann, and A. Javili, "Extended general interfaces: Mori–Tanaka homogenization and average fields," International Journal of Solids and Structures, vol. 254-255, p. 111933, 2022.

[25] K. Meski, B. Mamen, and A. Menasria, "Analytical solutions for the thermo-mechanical bending of FG beams using a higher order shear deformation theory (HSDT)," MATEC Web of Conferences, vol. 394, p. 03004, 2024.

[26] A. Chikh, "Analysis of static behavior of a P-FGM Beam," Journal of Materials and Engineering Structures, vol. 6, pp. 513–524, 2019.

[27] M. Chitour, B. Rebai, K. Mansouri, F. Khadraoui, A. Berkia, and T. Messas, "Investigating the influence of material composition on bending analysis of functionally graded beams using a 2D refined theory," Journal of Computational Applied Mechanics, vol. 55, no. 1, pp. 62–76, 2024.

[28] P. Bridjesh, G. C. Mohana Reedy, N. K. Geetha, C. Ravikiran, and S. Nagaraju, "On numerical bending analysis of functionally graded porous beam – Effect of porosity adapting higher order shear deformation theory," Journal of Computational Applied Mechanics, vol. 54, no. 1, pp. 49–67, 2023.

[29] G. C. M. Reddy, S. Valiveti, S. Hussain, and P. Bridjesh, "Comparative investigation of deflection in a two-directional functionally graded porous curved and straight beams adapting unified shear deformation theory," Journal of Computational Applied Mechanics, vol. 56, no. 1, pp. 145–161, 2025.

[30] X. Tang, Y. Zhang, J. Xu, J. Rutqvist, M. Hu, Z. Wang, and Q. Liu, "Determining Young's modulus of granite using accurate grain-based modeling with microscale rock mechanical experiments," International Journal of Rock Mechanics and Mining Sciences, vol. 157, p. 105167, 2022.

[31] J. A. TrustGod, O. S. Obinna, and N. Ebuka, "Characterized indices of bond thickness variation on RC beams strengthened externally by bonded carbon FRP," Nigerian Journal of Industrial and Professional Engineering Sciences, vol. 4, no. 4, pp. 1-10, Nov. 2022.

[32] U. N. Wilson, J. E. Sani, J. A. Sadiq, M. T. Abdulwahab, P. Abubakar, and R. O. Rahmon, "Investigating the effect of flexural strength of I and box African birch built-up beam on nail spacing," Nigerian Journal of Industrial and Professional Engineering Sciences, vol. 4, no. 4, pp. 1-10, Nov. 2022.

[33] C. C. Ike, "Static flexure of first order shear deformable thick beam resting on two-parameter elastic foundation – equilibrium formulation and closed form solutions," Nigerian Journal of Industrial and Professional Engineering Sciences, vol. 7, no. 1, pp. 1-10, Feb. 2025.

[34] C. Ike and J. N. Ugwu, "First principles Ritz variational formulation for buckling analysis of polynomial shear deformable beams: Analytical solutions," Nigerian Journal of Industrial and Professional Engineering Sciences, vol. 7, no. 3, pp. 1-10, Aug. 2025.

[35] C. C. Ike, "Static flexure of first order shear deformable thick beam resting on two-parameter elastic foundation – equilibrium formulation and closed form solutions," Nigerian Journal of Industrial and Professional Engineering Sciences, vol. 7, no. 1, pp. 1-10, Feb. 2025.

[36] F. Turan, M. F. Basoglu, and V. N. V. Hoang, "Lateral torsional stability of porous thin-walled I-beams with nonuniform porosity distributions subjected to a uniformly distributed load," Acta Mechanica, vol. 236, no. 1, pp. 153-171, 2025.

[37] F. Turan, "Critical lateral-torsional buckling loads of porous orthotropic rectangular beams containing warping effects," ZAMM-Journal of Applied Mathematics and Mechanics/Zeitschrift für Angewandte Mathematik und Mechanik, vol. 104, no. 12, e202400478, 2024.

[38] A. Doicheva, "Distribution of forces in RC interior beam–column connections," Engineering Proceedings, vol. 56, no. 1, p. 114, 2023.

[39] A. Doicheva, "Finite element method for analysis of off-center connected continuous beams," The Eurasia Proceedings of Science, Technology, Engineering & Mathematics (EPSTEM), vol. 18, pp. 37-45, 2022.

[40] Y. Gao, S. P. Xu, and B. S. Zhao, "Boundary conditions for elastic beam bending," Comptes Rendus. Mecanique, vol. 335, no. 1, pp. 1-6, 2007.

[41] Y. Gao, S. Xu, and B. Zhao, "Boundary conditions for the bending of a piezoelectric beam," Science in China Series G: Physics, Mechanics and Astronomy, vol. 51, no. 7, pp. 847-856, 2008.

[42] M. A. Biot, "Bending of an infinite beam on an elastic foundation," Journal of Applied Mechanics, vol. 4, no. 1, pp. A1-A7, 1937.

[43] S. P. Xu, "An operational calculus-based approach to a general bending theory of nonlocal elastic beams," European Journal of Mechanics-A/Solids, vol. 46, pp. 54-59, 2014.

[44] Y. M. Yue, K. Y. Xu, and T. Chen, "A micro scale Timoshenko beam model for piezoelectricity with flexoelectricity and surface effects," Composite Structures, vol. 136, pp. 278-286, 2016.

[45] X. Liu, J. Li, G. Tzimiris, and T. Scarpas, "Modelling of five-point bending beam test for asphalt surfacing system on orthotropic steel deck bridges," International Journal of Pavement Engineering, vol. 22, no. 11, pp. 1469-1490, 2021.

[46] X. Wang, K. Sun, J. Shao, and J. Ma, "Fracture properties of graded basalt fiber reinforced concrete: Experimental study and Mori-Tanaka method application," Construction and Building Materials, vol. 398, p. 132510, 2023.

[47] Y. Li, Y. Li, and R. Wang, "Quantitative evaluation of elastic modulus of concrete with nanoindentation and homogenization method," Construction and Building Materials, vol. 212, pp. 295-303, 2019.

[48] W. R. da Silva, J. Němeček, and P. Štemberk, "Application of multiscale elastic homogenization based on nanoindentation for high performance concrete," Advances in Engineering Software, vol. 62, pp. 109-118, 2013.

[49] J. Zhou, H. Lin, K. Qiu, K. Ou, and F. Nie, "Prediction of modulus of elasticity of concrete using different homogenization methods," Materials, vol. 18, no. 12, p. 2674, 2025.

[50] Y. Li, Y. Liu, and R. Wang, "Evaluation of the elastic modulus of concrete based on indentation test and multi-scale homogenization method," Journal of Building Engineering, vol. 43, p. 102758, 2021.

Authors' Contribution

Both authors contributed equally to the development of this article.

Data availability

All datasets relevant to this study's findings are fully available within the article.

How to cite this article (APA):

Ahmed, B., Hafida, D., Djihad, R., & Abdelmoutalib, B. (2025). FLEXURAL PERFORMANCE OF CONCRETE BEAMS INCORPORATING GRANITE WASTE. *Veredas Do Direito*, *22*(2), e3155. https://doi.org/10.18623/rvd.v22.n2.3155